Supplementary Information (SI) for Physical Chemistry Chemical Physics.
This journal is © the Owner Societies 2024

Supplementary Information

Ab-initio Study of Temperature-dependent Piezoelectric and Electronic Properties of Thermally Stable $GaPO_4$

Xiaoqing Yang,[1,2] Pan Guo,[2] Shunbo Hu,[2] Zhibin Gao,[3] Wenliang Yao,[2] Jinrong Cheng,[2] Samuel Poncé,[4,5] Baigeng Wang,[1] and Wei Ren[2*]

[1]*School of Physics and National Laboratory of Solid State Microstructures, Nanjing University, Nanjing 210093, China*

[2]*Physics Department, Materials Genome Institute, State Key Laboratory of Advanced Special Steel, Shanghai Key Laboratory of High Temperature Superconductors, International Centre for Quantum and Molecular Structures, Shanghai University, Shanghai 200444, China*

[3]*State Key Laboratory for Mechanical Behavior of Materials, Xi'an Jiaotong University, Xi'an 710049, China*

[4]*European Theoretical Spectroscopy Facility, Institute of Condensed Matter and Nanosciences, Université catholique de Louvain, Chemin des Étoiles 8, B-1348 Louvain-la-Neuve, Belgium*

[5]*WEL Research Institute, avenue Pasteur, 6, 1300 Wavre, Belgique*

Email: renwei@shu.edu.cn

Table S1 Band gaps (in eV) with lattice expansion (LE) effect, phonon vibration (VIB) effect and both of them are given at different temperatures.

	0 K_no ZPR	0 K_with ZPR	200 K	400 K	600 K	800 K	1000 K
LE	4.555	/	4.553	4.546	4.538	4.530	4.523
VIB	/	4.041	3.882	3.610	3.323	3.041	2.770
LE+VIB	/	3.719	3.556	3.266	2.959	2.659	2.374

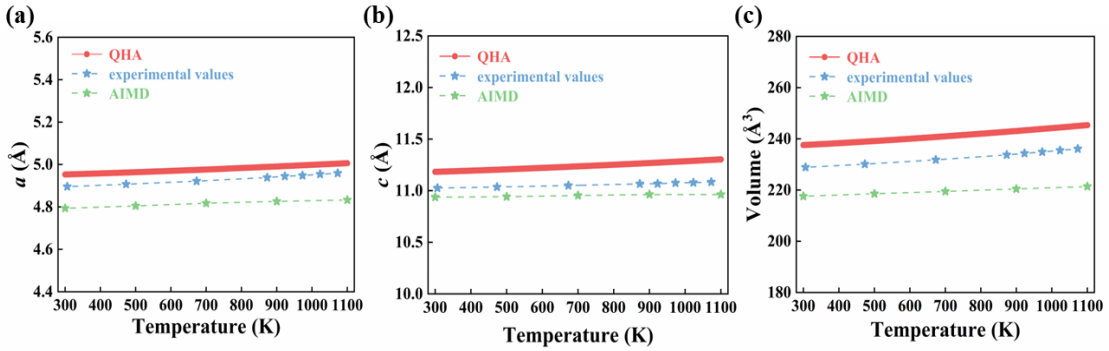

Fig. S1 Simulations for α-$GaPO_4$ at high temperatures (300 – 1100 K) for (a) lattice constant a, (b) lattice constant c and (c) volume. The red line is obtained by the quasi-harmonic approximation (QHA) method. The blue star symbols represent experimental data[1] and the green ones are obtained by *ab initio* molecular dynamics (AIMD) simulations for 20 ps with a time step of 2 fs.

Table S2 Elastic stability criteria for the mechanically stable crystal $GaPO_4$.

(i)	$C_{11} > C_{12}$
(ii)	$2C_{13}^2 < C_{33}(C_{11} + C_{12})$
(iii)	$2C_{14}^2 < C_{44}(C_{11} - C_{12})$
(iv)	$C_{44} > 0$

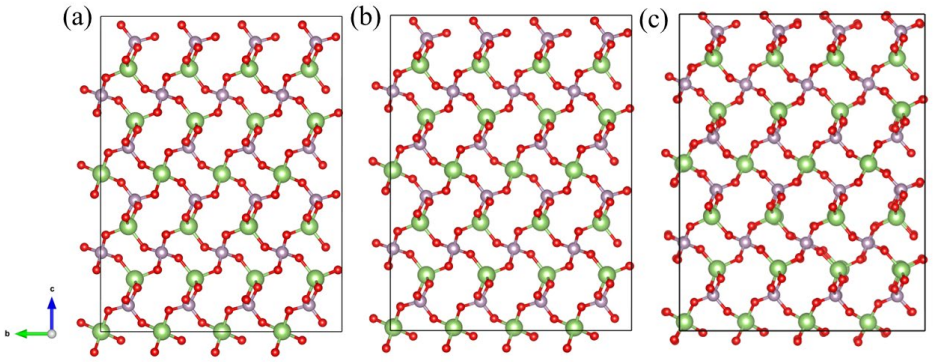

Fig. S2 Snapshots of α-$GaPO_4$ 4×4×2 supercell at (a) 300 K, (b) 700 K and (c) 1000 K after 20 ps AIMD simulations in the isothermal-isobaric (NPT) ensemble using a Langevin thermostat.

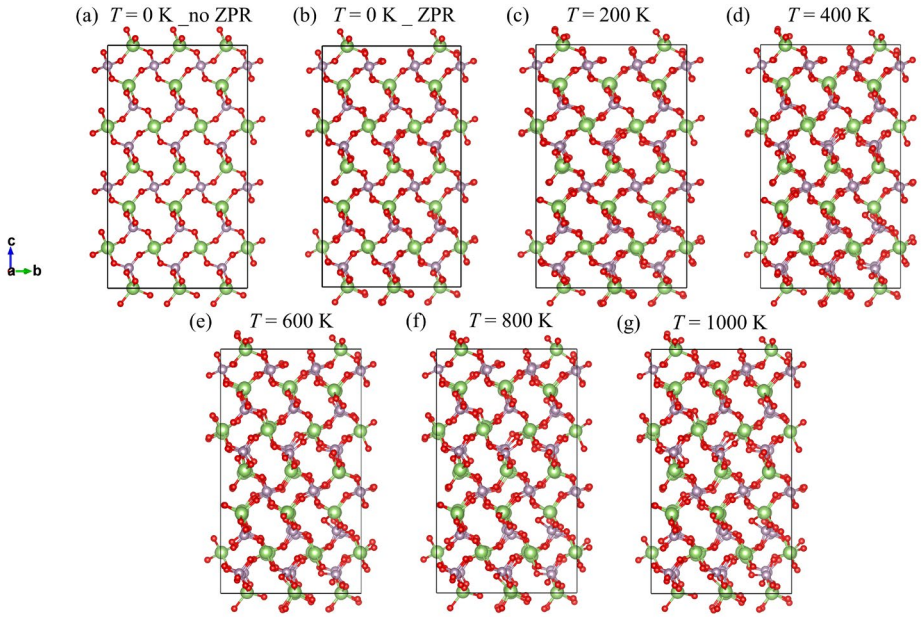

Fig. S3 (a) Snapshots of α-$GaPO_4$ 3×3×2 supercell excluding the electron-phonon interaction and thus without zero-point renormalization (ZPR), and configurations including electron-phonon interaction at (b) 0 K with ZPR, (c) 200 K, (d) 400 K, (e) 600 K, (f) 800 K and (g) 1000 K.

$$e_{ik} = \begin{bmatrix} e_{11} & -e_{11} & 0 & e_{14} & 0 & 0 \\ 0 & 0 & 0 & 0 & -e_{14} & -2e_{11} \\ 0 & 0 & 0 & 0 & 0 & 0 \end{bmatrix} \tag{S1}$$

$$C_{kj} = \begin{bmatrix} C_{11} & C_{12} & C_{13} & C_{14} & 0 & 0 \\ C_{12} & C_{11} & C_{13} & -C_{14} & 0 & 0 \\ C_{13} & C_{13} & C_{33} & 0 & 0 & 0 \\ C_{14} & -C_{14} & 0 & C_{44} & 0 & 0 \\ 0 & 0 & 0 & 0 & C_{44} & C_{14} \\ 0 & 0 & 0 & 0 & C_{14} & C_{66} \end{bmatrix} \tag{S2}$$

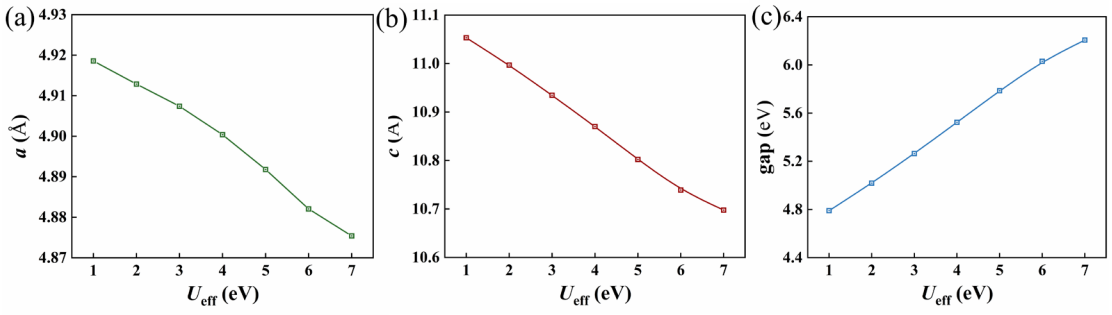

Fig. S4 The Hubbard U_{eff} dependences of (a) lattice a, (b) lattice c and (c) band gap for $GaPO_4$.

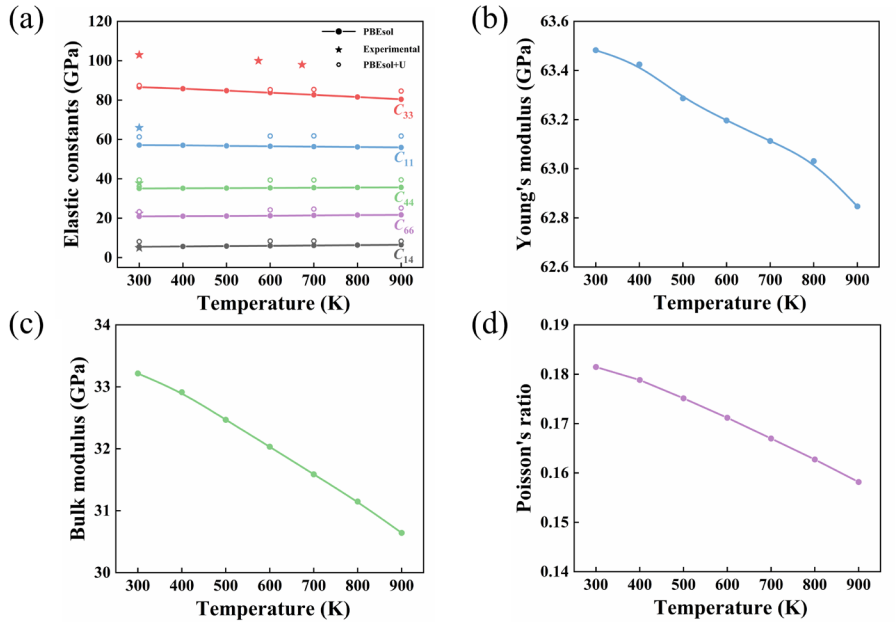

Fig. S5 Temperature-dependent (a) elastic constants, (b) Young's modulus, (c) bulk modulus, and (d) Poisson's ratio. The star symbols in (a) represent the experimental data[2]. The hollow circle symbols are calculated by PBEsol+U (U_{eff} = 2 eV for Ga atoms).

Elastic modulus is one of the key properties in materials engineering and mechanics. Studying the effect of temperature on elastic modulus is particularly important for the application of high-temperature materials. According to the generalized Hooke's law, the four material parameters of elasticity in Fig. S5 can describe the reaction of materials when a load is applied, and the energy is a quadratic function of these parameters. The premise of obtaining a stable equilibrium point is that the quadratic form of the energy must be positive and definite, which imposes conditions on the elastic constant. Fig. S5(a) shows the predicted values for C_{11}, C_{33}, C_{14}, C_{44}, C_{66} compared to experimental data at different temperatures. The predicted elastice constants C_{ij} evolve smoothly with temperature, which comply with the stability criteria (in Table S2), confirming that α-$GaPO_4$ remains mechanically stable even at high temperatures. The predicted elastic constants C_{14}, C_{44}, C_{66} coincide with the experimental data well at room temperature, while the predicted C_{11} and C_{33} deviate from the experimental data when Hubbard U effect is not considered. One can note that the QHA simulation overestimates volume expansion with increasing temperature, as shown in Fig. S1. Since the elastic constants C_{11} and C_{33} decrease over volumetric expansion, the overestimated lattice parameters a and c would lead to underestimated C_{11} and C_{33} values.

The PBEsol+*U* method provides finer predictions to the lattice constants as compared to the experimental results (as shown in Table S3). It indeed provides finer predictions of C_{11} to the experimental value, while having little effect on C_{33}.

Table S3 Lattice constants (Å) and volume (Å^3) with different functionals (at 0 K) and experimental values of $GaPO_4$.

	Functional	PBE	LDA	PBEsol	PBEsol+*U*	experiment
$GaPO_4$	$a = b$	5.01	4.82	4.91	4.91	4.92
	c	11.26	10.95	11.10	11.00	11.00
	V	244.66	220.47	232.09	229.86	230.60

The value of Young's modulus is often required for engineering designs of micro-electro-mechanical systems (MEMS) technology. Young's modulus can quantify and describe tensile elasticity or the tendency of an object to deform along an axis when opposing forces are applied along this particular axis, reflecting the stiffness of materials. Fig. S5(b) shows that the Young's modulus of $GaPO_4$ decreases slowly, with a change of only 0.73 GPa from 300 K to 1000 K. Bulk modulus is a vital physical parameter for advanced high-performance materials. It reflects the internal bonding character of atoms and the resistance of the material to volume change. We find that the bulk modulus of $GaPO_4$ decreases only by 3 GPa upon heating, and its softening resistance is strong. The bulk modulus of $GaPO_4$ thus presents better thermal stability than $AlPO_4$[3]. Poisson's ratio is a specific value that describes the lateral deformation of a material. Fig. S4(d) displays that the Poisson's ratio of $GaPO_4$ is in the range of common materials and similar to that of SiO_2 (0.17)[4]. At elevated temperatures, the Poisson's ratio decreases accompanied by greater brittleness and better resistance to lateral deformation. In general, $GaPO_4$ turns out to be a typical brittle material with strong compressive strength, suitable for stable application in a high-temperature environment.

Table S4 Piezoelectric constants e_{ij} (C/m^2), elastic constants C_{ij} (GPa) and piezoelectric modulus d_{ij} (pC/N) of APO_4 (A=B, Al, Ga, In).

Piezoelectric constants (C/m^2)	BPO_4	$AlPO_4$	$GaPO_4$	$InPO_4$
$e_{11,i}$	0.37	0.30	0.43	0.62
$e_{11,c}$	-0.25	-0.15	-0.24	-0.28
e_{11}	0.12	0.15	0.18	0.35
e_{14}	0.03	0.03	0.13	-0.01
C_{14}	9.89	11.93	4.27	0.16
C_{33}	234.42	87.03	97.73	68.04
C_{44}	113.41	42.85	35.25	11.93
C_{66}	68.26	28.76	21.33	8.56
d_{11}	0.89	2.68	3.98	20.30
d_{14}	0.12	-0.78	3.18	-1.26

Table S5 Piezoelectric constants e_{ij} (C/m^2) with different functionals (at 0 K) and experimental values of APO_4.

	Functional	PBE	LDA	PBEsol	PBEsol+U	other[1, 5, 6]
BPO_4	e_{11}	0.11	0.13	0.12	/	0.11
	e_{14}	0.01	0.04	0.03		0.02
$AlPO_4$	e_{11}	0.13	0.17	0.15	/	0.14
	e_{14}	0.01	0.05	0.03		0.02
$GaPO_4$	e_{11}	0.17	0.20	0.18	0.17	0.21
	e_{14}	0.11	0.11	0.13	0.04	0.10
$InPO_4$	e_{11}	0.28	0.46	0.35	0.30	/
	e_{14}	0.09	-0.63	-0.01	0.01	

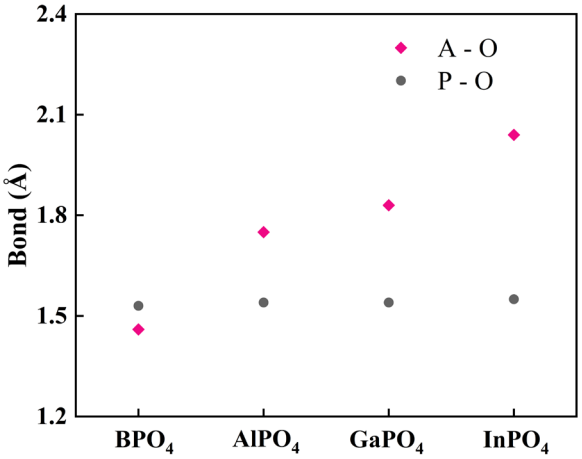

Fig. S6 Bond length for APO_4 (A=B, Al, Ga, In). Pink dots are bonds between A and O, gray dots are bonds between P and O.

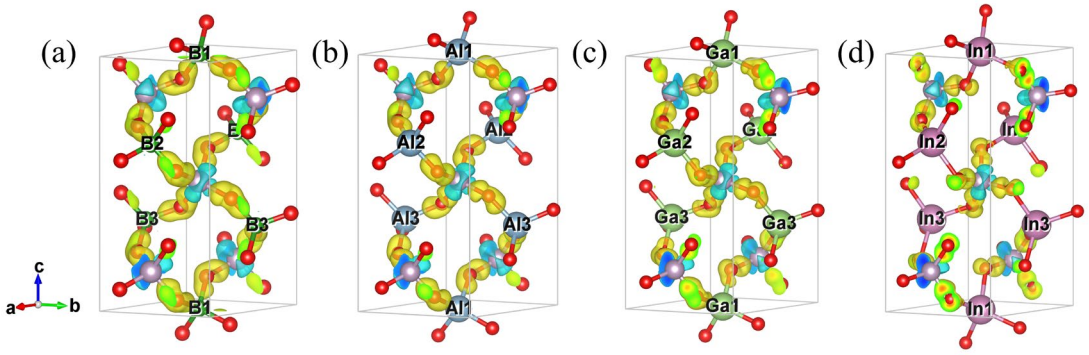

Fig. S7 Charge density difference of (a) BPO_4, (b) $AlPO_4$, (c) $GaPO_4$ and (d) $InPO_4$. Isosurfaces level is set as ±0.027, with yellow and blue regions for charge cumulation and depletion, respectively. Red and purple spheres represent O and P atoms, respectively.

Following is about the piezoelectricity of α-$GaPO_4$ as the temperature rises to 1000 K. There are two significant angles that link to the structural distortion of the piezoelectric α-phase in Fig. S8(a). One is the inter-tetrahedral bridging angle θ of Ga-O-P, while the other is the tilt angle δ that reflects the degree of tetrahedral rotated distortion. The tilting δ becomes 0 when transforming to β-phase, accompanied by the disappearance of piezoelectricity. The tilt angle δ is also directly related to the bridging angle θ with the following relationship[7]:

$$\cos\theta = \frac{3}{4} - \left(\cos\delta + \frac{1}{2\sqrt{3}}\right)^2. \quad \text{(S3)}$$

Fig. S8(b) shows the evolution of bridging angle θ and tilt angle δ as a function of temperature from 300 K to 1000 K. These two angles weakly depend on temperature. The bridging angle θ increases slowly by about 2° as the temperature increases by 700 K. Similarly, the tilt angle δ lowers slowly as a function of temperature, indicating that the geometry of α-$GaPO_4$ remains distorted at high temperatures and is thus thermally stable. This feature of α-$GaPO_4$ is different from α-SiO_2, whose tilt angle δ drops fast when the temperature rises[8]. Therefore, α-$GaPO_4$ crystal has far more profound high-temperature thermal stability than α-SiO_2 and is suitable to work in a wide temperature range.

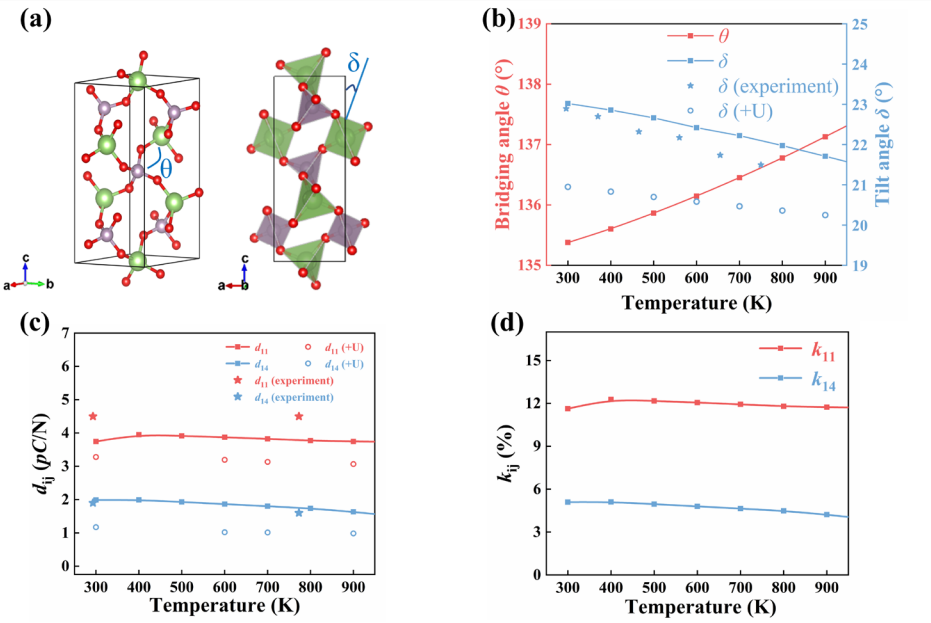

Fig. S8 (a) The inter-tetrahedral bridging angle θ of Ga-O-P and the tilt angle δ related to the rotation angle between α-$GaPO_4$ and β-$GaPO_4$. The green and gray tetrahedral are GaO_4 and PO_4, respectively. (b) Dependence between the calculated angles (θ and δ) and the temperature, the star symbols are experimental data of δ[8]. (c) Piezoelectric modulus d_{11} and d_{14} as a function of the temperature. (d) The temperature dependence of the electromechanical coupling coefficient k_{11} and k_{14}. The solid points are calculated by PBEsol without Hubbard U, and the hollow circle is calculated by PBEsol+U (U_{eff} = 2 eV).

The degree of structural distortion has a direct impact on piezoelectric properties. The crystal of α-$GaPO_4$ has only two independent piezoelectric constants displayed in Equation S1: e_{11} and e_{14}. Piezoelectric modulus d_{ij} reflects the ability to transform between the mechanical and electrical energy. To investigate the piezoelectric behavior during the temperature change, we calculate d_{ij} based on first principles and QHA, from which d_{ij} can be obtained through the thermodynamic relationship between e_{ik} and S_{kj} matrices. The elastic compliance tensor S_{kj} is the inverse matrix of elastic constants C_{kj} (Equation S2), and relates to the deformation produced by the application of a stress. Eventually, d_{11} and d_{14} can be expressed as:

$$d_{11} = e_{11}(S_{11} - S_{12}) + e_{14}S_{14}, \quad \text{(S4)}$$

$$d_{14} = 2e_{11}S_{14} + e_{14}S_{44}. \quad \text{(S5)}$$

The d_{11} and d_{14} values as a function of temperature are reported in Fig. S8(c). d_{11} is almost independent from temperature and the general trend is consistent with experiment, although our results

are about 16% smaller than the measured data[9]. d_{14} decreases slightly from 2.0 pC/N to 1.5 pC/N over this temperature interval, which agrees well with the experimental value. The piezoelectric modulus d_{11} and d_{14} are also calculated by PBEsol + U (U_{eff} = 2 eV), which deviate significantly from the experimental results.

The electromechanical coupling coefficient k_{ij} defined as $k_{ij}=d_{ij}/(\varepsilon_{ii}S_{jj})^{-1/2}$ is another important indicator of piezoelectric materials, which suggests their ability to convert electrical energy into mechanical quantities and vice versa and whether it is suitable for designing energy harvesting and sensing transducers[10]. $GaPO_4$ possesses more advantages compared with quartz, such as higher d_{11} and k_{11}, and higher critical temperature up to 1206 K, at which temperature an irreversible transformation into a cristobalite-like phase occurs. Therefore, it is an excellent material for use as a pressure transducer and other functional applications that involve harsh high-temperature environments.

References

1. Haines, J.; Cambon, O.; Prudhomme, N.; Fraysse, G.; Keen, D. A.; Chapon, L. C.; Tucker, M. G., High-temperature, structural disorder, phase transitions, and piezoelectric properties of $GaPO_4$. *Physical Review B* **2006,** *73* (1), 014103.
2. Armand, P.; Beaurain, M.; Ruffle, B.; Menaert, B.; Balitsky, D.; Clement, S.; Papet, P., Characterizations of piezoelectric $GaPO_4$ single crystals grown by the flux method. *Journal of Crystal Growth* **2008,** *310* (7-9), 1455-1459.
3. Wang, R.; Kanzaki, M., Phase diagram and thermodynamic properties of $AlPO_4$ based on first-principles calculations and the quasiharmonic approximation. *Physics and Chemistry of Minerals* **2014,** *42*, 15-27.
4. Irzaman; Oktaviani, N.; Irmansyah, Ampel bamboo leaves silicon dioxide (SiO_2) extraction. *IOP Conference Series: Earth and Environmental Science* **2018,** *141* (1), 012014.
5. SHAFER, E. C.; ROY, R., Studies of Silica-Structure Phases: I, $GaPO_4$, $GaAsO_4$, and $GaSbO_4$. *Journal of the American Ceramic Society* **1956,** *39* (10), 330-336.
6. Hermet, P.; Haines, J.; Aubry, J. P.; Cambon, O., Origin and mechanism of piezoelectricity in α-Quartz-type $M^{III}X^{V}O_4$ Compounds (M = B, Al, or Ga; X = P or As). *The Journal of Physical Chemistry C* **2016,** *120* (47), 26645-26651.
7. Labéguerie, P.; Harb, M.; Baraille, I.; Rérat, M., Structural, electronic, elastic, and piezoelectric properties of α-quartz and MXO_4 (M=Al, Ga, Fe; X=P, As) isomorph compounds: A DFT study. *Physical Review B* **2010,** *81* (4), 045107.
8. Haines, J.; Cambon, O.; Rouquette, J.; Bornand, V.; Papet, P.; Leger, J.; Hull, S., Neutron and X-ray diffraction studies of piezoelectric materials under non-ambient conditions. *Materials Science Forum* **2004,** *443*, 277-282.
9. Worsch, P.; Krempl, P.; Krispel, F.; Reiter, C.; Thanner, H.; Wallnoefer, W., The temperature-stable piezoelectric material $GaPO_4$ and its sensor applications. *Transducers 01 Eurosensors XV* **2001**, 978-981.
10. Yu, K.; Liu, T. Calculation of electromechanical coupling coefficient of quartz crystal in decoupling plane, *Proceedings of SPIE - The International Society for Optical Engineering*, 2010.